ORIGINAL PAPER

S. S. Zhang · M. H. Ervin · D. L. Foster · K. Xu
T. R. Jow

Fabrication and evaluation of a polymer Li-ion battery with microporous gel electrolyte

Abstract This paper introduces an easy method for the fabrication of polymer Li-ion batteries with microporous gel electrolyte (MGE). The MGE is a multiphase electrolyte, which is composed of liquid electrolyte, gel electrolyte, and polymer matrix. The MGE not only has high ionic conductivity and good adhesion to the electrodes at low temperatures, but also retains good mechanical strength at elevated temperatures. Therefore, the MGE batteries are able to operate over a wide temperature range. During battery fabrication, the MGE is formed in situ by introducing liquid electrolyte into a swellable microporous polymer membrane and then heating or cycling the battery. In this work, the chemical compatibility of MGE with metal lithium during 60 °C storage and with $LiMn_2O_4$ cathode during cycling was studied. In addition, graphite/MGE/$LiMn_2O_4$ Li-ion batteries were made and evaluated.

Keywords Microporous gel electrolyte · Microporous membrane · Gel polymer electrolyte · Phase inversion · Polymer Li-ion battery

Introduction

Applications of conventional gel polymer electrolyte (GPE) as a separator in rechargeable batteries are limited to near ambient temperatures. At elevated temperatures, the GPE becomes a viscous fluid, so its mechanical strength is dramatically decreased. As a result, the GPE loses its separating ability and the battery short-circuits internally. Previous solutions to this problem have included mixing inorganic filler, such as zeolite, alumina, and silica, into the polymer matrix [1, 2, 3] and coating the GPE onto a porous polyolefin membrane/cloth [4, 5, 6]. Furthermore, fabrication of

S. S. Zhang (✉) · M. H. Ervin · D. L. Foster · K. Xu · T. R. Jow
U.S. Army Research Laboratory,
Adelphi, MD 20783–1197, USA
E-mail: szhang@arl.army.mil

the GPE is inconvenient because it involves the use of highly hydroscopic lithium salt and organic solvents, which require an anhydrous environment [1, 2, 3, 4, 5, 6, 7, 8]. To resolve the above problems, Telcordia (formerly Bellcore) researchers developed an improved process, in which a plasticizer with a high boiling point is first mixed into the polymer matrix to create a porous structure and then a liquid electrolyte is introduced to swell the polymer [9, 10]. This approach offers the advantage of allowing the battery to be assembled in a non-anhydrous environment. However, it requires an additional procedure of extracting the plasticizer, which increases the cost of battery fabrication.

With this in mind, we introduced microporous gel electrolyte (MGE), which is composed of a porous solid polymer matrix filled with both GPE and liquid electrolyte [11]. The MGE not only has high conductivity at low temperature but it also retains stable dimensions at elevated temperature. The MGE is easily prepared by wetting a swellable microporous separator with the liquid electrolyte and leaving it to gel. Therefore, the MGE technique allows the electrolyte activation to be carried out in the last step of the battery assembly, which greatly simplifies production. In this work, we report the fabrication and performance of MGE-based MCMB/$LiMn_2O_4$ Li-ion batteries.

Experimental

Kynar Flex 2801, a poly(vinylidene fluoride-co-hexafluoropropylene) copolymer from Elf Atochem North America, was used as the polymer matrix for the MEG. Microporous membranes were prepared by the phase inversion method with acetonitrile (AN) and N-methyl pyrrolidinone (NMP), respectively, as the polymer solvent. Kynar powder was dissolved into the solvent to make a 20 wt% solution by stirring and heating at 60 °C. The warm polymer solution was cast onto a Teflon-coated substrate using a doctor blade with a gap of 0.24 mm. The resulting dope was immediately

immersed into a coagulation bath filled with deionized water to precipitate the polymer. Due to the fast exchange between the solvent and coagulation medium, a microporous membrane was formed in seconds and then peeled off the substrate. The obtained membrane was dried at 90 °C under vacuum for 16 h and cut into small discs of 2.85 cm^2 (diameter = 0.75 inch) for future characterization and use.

A solution of 1.0 m LiBF$_4$ dissolved in a 1:3 (wt.) mixture of ethylene carbonate (EC) and γ-butyrolactone (GBL) was used as the liquid electrolyte. The MEG was prepared by dipping microporous membrane into the liquid electrolyte for 1 day in spite of the fact that the liquid electrolyte could rapidly penetrate into the porous membrane. After wetting, the membrane was lightly pressed between two sheets of filter paper to remove the excess liquid electrolyte on the surface, and then was heated to 80 °C for 20 min to promote formation of the MGE. Generally, the porous membrane could take up 120 ± 5 wt% of liquid electrolyte versus the weight of the dried membrane, and the swollen membrane has a thickness of 0.14 mm. To measure ionic conductivity, the swollen membrane was sandwiched between two stainless steel plates and sealed in a 2325-type button cell. The conductivity was calculated from the impedance of the cell.

Electrode films of LiMn$_2$O$_4$ and MCMB (mesophase carbon micro beads), supplied by E-One Moli Energy (Canada), were used to evaluate the performance of the MGE Li-ion cells. The electrode sizes were 0.97 cm^2 for the cathode and 1.27 cm^2 for the anode. The anode, dried membrane, and cathode were stacked sequentially into a button cell can, and activated by filling with 150 μm of liquid electrolyte. After sealing, the cell was heated to 80 °C for 20 min to promote formation of the MGE, and then it was formed (pre-conditioned) and tested on a Maccor Series 4000 tester. Testing conditions are described in detail either in the text or in the figure caption.

A Tenney Environmental Oven Series 942 was used to control the temperatures of the cells. A Solartron SI 1287 Electrochemical Interface and a SI 1260 Impedance/Gain-Phase Analyzer were employed to measure impedance. For conductivity measurement, the impedance was measured over the frequency range of 100 kHz to 1 Hz with an AC oscillation of 10 mV. For cell evaluation, the impedance was measured potentiostatically by applying a DC bias (its value equal to the open-circuit voltage of the cell) and an AC oscillation of 10 mV over the frequency range of 100 kHz to 0.01 Hz. The impedance spectra obtained were fitted using ZView software.

Results and discussion

Fabrication and ionic conductivity of the MGE

Porous Kynar membranes were prepared by the phase inversion method using AN and NMP, respectively, as the solvent and water as the non-solvent. Formation of the porous structure by this method is based on a fast exchange between the solvent and the non-solvent, the so-called coagulation medium, in the polymer solution. The morphology of the membrane made in this way is affected by many factors, including the type of solvent and non-solvent, concentration and temperature of the polymer solution, thickness of the polymer dope, and so forth. It has been reported that membranes made by the phase inversion method are structurally asymmetric, mostly being composed of a highly porous body with a very dense skin on each side of the membrane [12, 13, 14]. Formation of the asymmetric structure is considered a result of the syneresis pressure, which spontaneously develops within the polymer solution and affects the nucleation and growth of the precipitated polymer [14]. However, in this work, we successfully prepared a membrane with an open pore structure, as shown in Fig. 1a and Fig. 1b. It is shown that the solvent significantly affects the texture of membrane pores. We see that the membrane formed with AN solvent has a flat surface (Fig. 1a), while the one formed with NMP solvent has a very rough surface (Fig. 1b). The open pores in both membranes certainly facilitate the penetration of the liquid electrolyte. We found that both membranes could be wetted rapidly and swollen slowly by many liquid electrolytes. After a limited swelling, the membrane was dried at 80 °C under vacuum, which left a membrane with much less porosity (Fig. 1c). The salts left randomly disperse in the pores and in the polymer cracks. This observation suggests that liquid, gel, and polymer solid phases coexist in the electrolyte-wetted porous membrane, so we called it "microporous gel electrolyte (MGE)". Without any supports, the MGE film is free-standing and retains good mechanical strength over a wide temperature range, which enables it to serve as the battery separator at elevated temperatures.

Due to the coexistence of the liquid and gel electrolyte, the MGE exhibits high conductivity. Typically, the MGE with a liquid electrolyte uptake of 120 ± 5 wt% (versus the weight of the dried membrane) has an ionic conductivity of 3.4 mS cm^{-1} versus 6.4 mS cm^{-1} of the liquid electrolyte at 20 °C and 0.4 mS cm^{-1} versus 1.0 mS cm^{-1} of the liquid electrolyte at −40 °C. The high conductivity of the MGE can be attributed to the presence of free liquid electrolyte in the pores of the membrane. The MGE batteries may be practically produced using a significantly simplified fabrication process. It can be completed briefly by three steps: (1) making the microporous membrane separator; (2) activating the battery with liquid electrolyte, and; (3) forming the MGE in situ by heating the battery to 80 °C or just cycling the battery. Due to the high melting point of Kynar materials, the porous structure of the membrane can withstand high temperatures, which facilitates the process of removing moisture from the battery stack (a necessary process before the electrolyte activation). Therefore, the MGE battery fabrication, except for the step of electrolyte activation, can be conducted in a non-anhydrous environment.
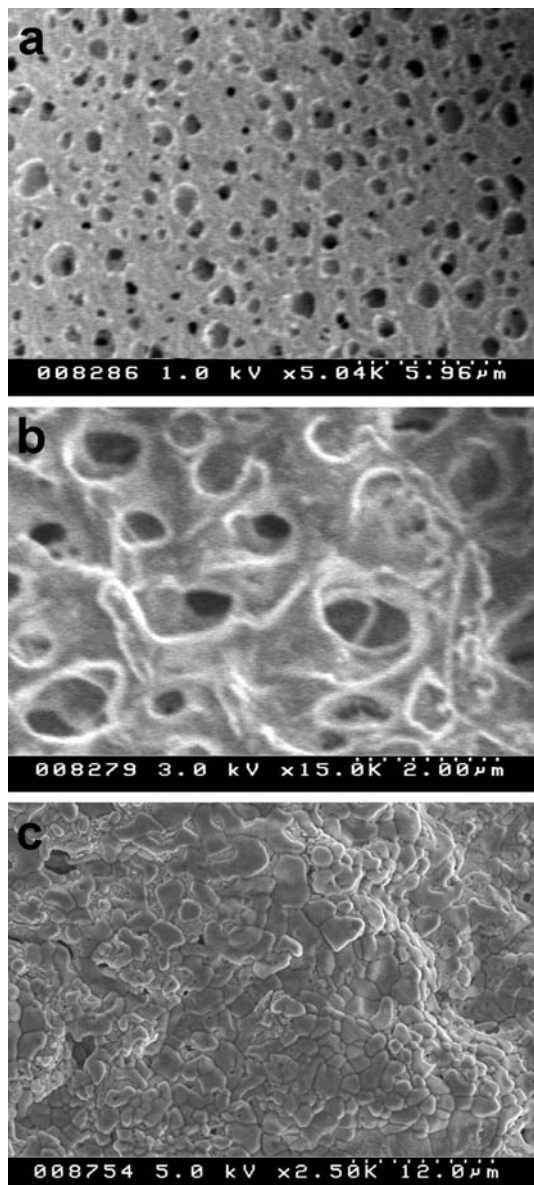
Fig. 1 SEM images of the membrane surface. **a** a membrane prepared with AN solvent; **b** a membrane prepared with NMP solvent; **c** a dried MGE

Fig. 2 Nyquist plots of a symmetric Li/MGE/Li cell for different storage times at 60 °C

Electrochemical stability of the MGE

Cathodic (reductive) stability of the MGE is evaluated by monitoring the impedance change of a symmetric Li/MGE/Li cell. Figure 2 compares Nyquist plots of the cell after storing at 60 °C for different times. The impedance spectrum of the MGE cell is composed of three overlapped semicircles. Such a pattern for the impedance spectrum can be fitted by an equivalent circuit, as shown in Fig. 3. R_b is the bulk resistance of the electrolyte, Z_p is impedance of the passivation layer on the surface of lithium metal, which consists of the resistance (R_p) of the passivation layer and its related capacitance (C_p), and Z_f is the Faradic impedance r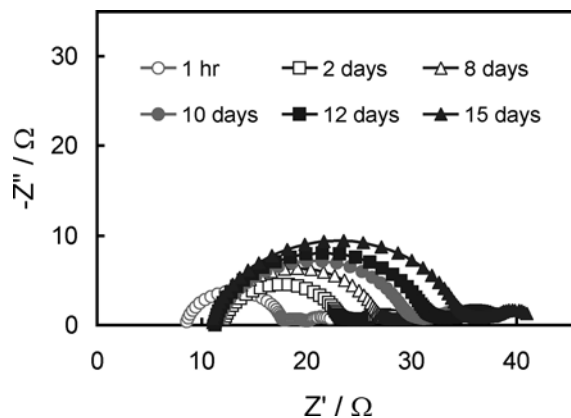eflecting the impedances of charge-transfer (Z_{ct}) and ion diffusion (Z_d) at the lithium-electrolyte interface. In some cases, two semicircles contributed by the charge-transfer and ion diffusion are merged with each other. This is due to the fast diffusion of Li$^+$ ions at the Li-MGE interface.

Based on Fig. 3, the R_b, R_p, and Z_f values were fitted and plotted as a function of the storage time in Fig. 4. It is shown that R_b sharply increased during the initial 15 h, and then slowly decreased from 15 to 11 ohms. Initially, the absorbed liquid electrolyte is immobilized in the pores of the membrane as liquid droplets, which contributes to the high conductivity of the membrane. With increasing storage time, the liquid electrolyte is gradually plasticized into the polymer matrix to form a gel electrolyte. Owing to consumption of the liquid electrolyte, some ion conduction pathways between the liquid droplets are broken off. As a result, the ionic conductivity of the membrane is decreased, which corresponds to a rapid increase in R_b. With increasing storage time, the swollen membrane undergoes a small amount of dimensional creep, which could cause a
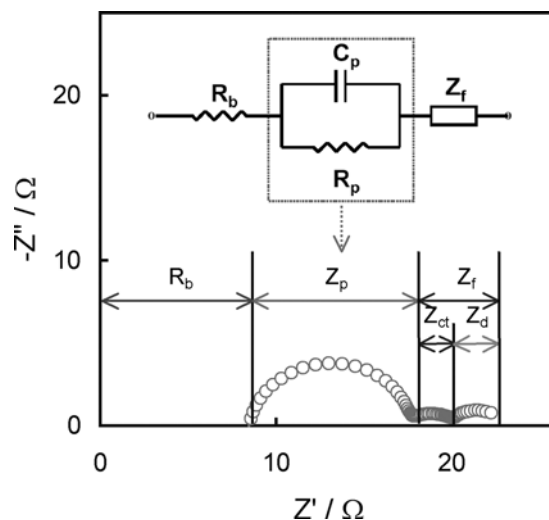

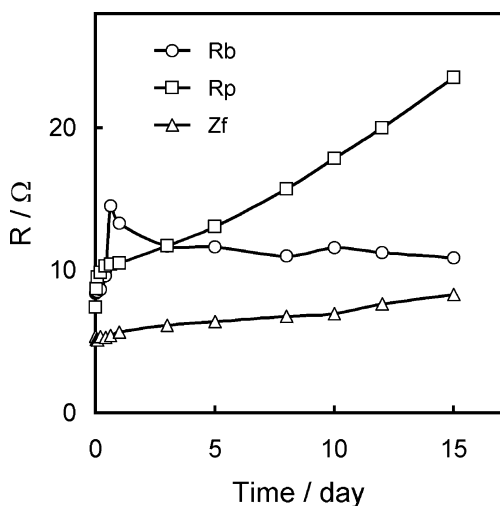**Fig. 3** Equivalent circuit used for analysis of the impedance spectra

Fig. 4 Time dependence of R_b, R_p, and Z_f for the Li/MGE/Li cell at 60 °C

Fig. 5 Anodic stability of the MGE with respect to the LiMn$_2$O$_4$ cathode

decrease in the thickness of the membrane. Therefore, we observed that R_b decreased slowly with extended storage time.

Conversely, both R_p and Z_f increased with storage time. R_p increased much faster than Z_f. In lithium batteries, the increase in R_p is inevitable due to the formation and progressive growth of the passivation layer on the lithium surface. The rapid increase of R_p in the initial few hours corresponds to the formation of the passivation layer, and the slow increase in the extended period to the growth of the resulted film. Therefore, the "R_p-t" response reflects the reactivity of the electrolyte components and the metal lithium. We noticed that the increase in R_p in the MGE cell is much slower than that observed from the liquid electrolyte counterpart. This improvement is attributed to the good stability of the MGE against the metal lithium. The slow and smooth increase in Z_f (Fig. 4) is likely a result of the combined effect of the changes in R_b and R_p. It should be mentioned that the data in Fig. 4 were measured without the use of a structural frame for the MGE. Success in this experiment has verified the good mechanical strength of MGE at 60 °C.

Figure 5 shows the anodic (oxidative) stability of the MGE, which was measured in a three-electrode Li/MGE/LiMn$_2$O$_4$ cell with a slow scanning rate of 0.02 V s^{-1}. First, we see that the cathode can be reversibly cycled between 3.5 V and 4.2 V with a high Coulomb efficiency of 92.2% (first cycle). Second, the anodic current falls back to the background level as the potential is increased to 4.3 V. This phenomenon indicates that, in the MGE, the cathode active material can be fully utilized without any oxidization of the MGE. Third, the anodic current stabilizes at the background until 4.9 V and remains at a low value with the anodic current showing a board peak as the potential is scanned toward the more positive direction. This implies that the Al current collector can be well passivated with the
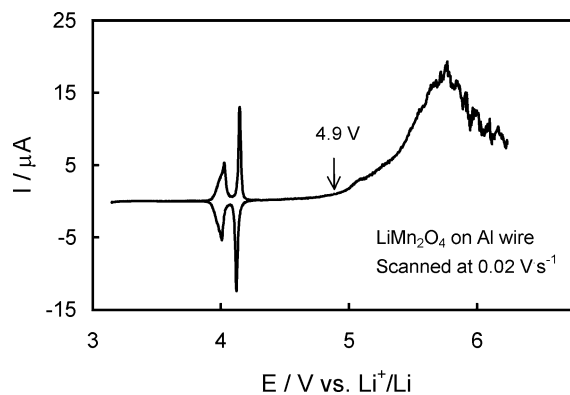
MGE, and that the MGE itself is stable on the surface of the passivated Al substrate.

Cycling performance of the MGE Li-ion cell

Figure 6 shows plots of differential capacities versus cell voltage for the first two cycles of a MGE Li-ion cell, in which the anode and cathode are respectively MCMB and LiMn$_2$O$_4$. It is shown that the Coulomb efficiency of the cell was 87.2% in the first cycle, and it increased to 97.5% in the second cycle. This feature indicates that a protective solid electrolyte interface (SEI) can be effectively formed with the MGE, which is known to be essential for the operation of Li-ion batteries.

Figure 7 compares the cycling performances of two identical MGE Li-ion cells, which were cycled at room temperature and at 60 °C, respectively. At room temperature, the capacity increased initially and then remained stable at ~1.90 mAh cm^{-2}. The initial increase in the capacity is likely associated with initial insufficient wetting of the electrodes so that the active materials cannot be fully utilized. At 60 °C, the cell started with
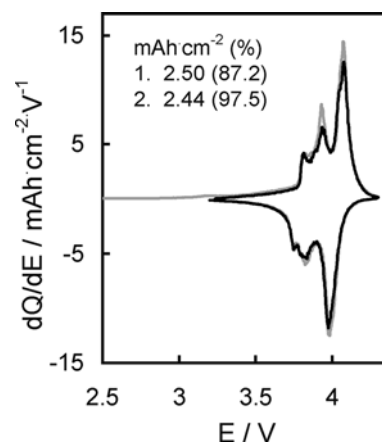

Fig. 6 Plots of differential capacity versus cell voltage for the first two cycles of the MGE Li-ion cell, which were recorded at 0.11 mA (C/20)
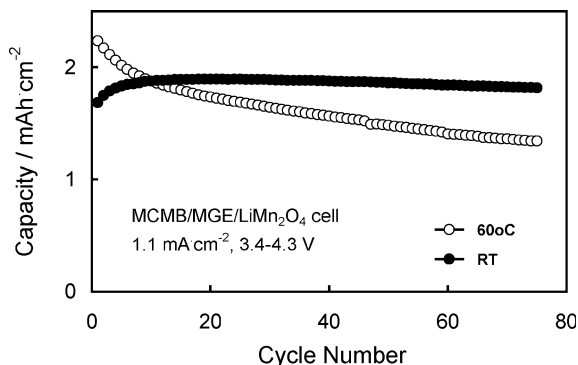
Fig. 7 Cycling performance of the MCMB/MGE/LiMn$_2$O$_4$ cell at room temperature and at 60 °C, respectively

higher capacities, but suffered fast capacity fading, which is most probably related to the LiMn$_2$O$_4$ cathode. The mechanisms identified for the capacity fading of LiMn$_2$O$_4$ cathodes are chemical dissolution [15, 16] and irreversible phase transition [17, 18], both of which result in structural degradation. Nevertheless, progressive cycling at 60 °C verifies that at elevated temperatures the MGE is able to serve as the battery separator where many GPE soften or even become viscous fluids unless they are mechanically strengthened by inorganic fillers [1, 2, 3] or supporting membranes [4, 5, 6].

The chemical compatibility of the MGE and the electrodes is evaluated by observing the impedance change of the MGE Li-ion cell under an overcharge condition. In a 60 °C oven, the cell was charged to 4.2 V and then constantly kept at 4.2 V for storage and impedance measurement.

Figure 8 shows Nyquist plots of the cell after storing at 60 °C for different times. Initially, two semicircles of the SEI and charge-transfer process are clearly distin-
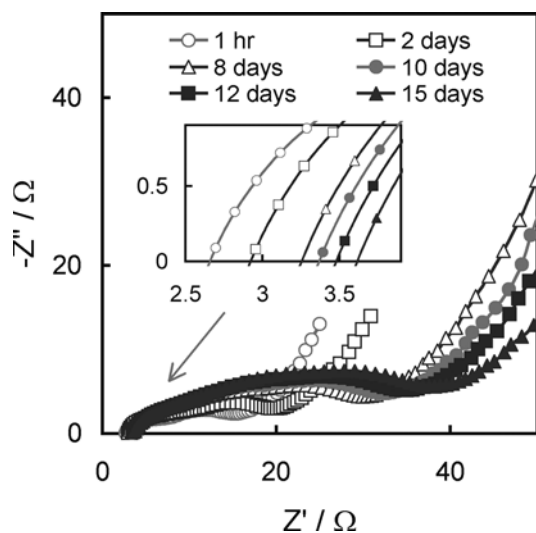
guished. With increasing storage time, both semicircles grow and gradually overlap each other. This behavior can be ascribed to the reactions of the electrolyte components and cathode active materials. As shown in the inset of Fig. 8, R_b gradually increases with the storage time, an opposite trend to that observed in Fig. 2. This is because the reactions consume liquid electrolyte, which consequently reduces the ionic conductivity of the MGE bulk. Meanwhile, non-conducting products of the reactions accumulate on the electrolyte-electrode interfaces, which physically block the processes of ion conduction and charge-transfer. This could be another reason for the increase in R_b. The above results suggest that chemical stability under the overcharge condition could be a challenge for the MGE.

Figure 9 shows discharge curves for the MGE Li-ion cell at low temperatures. In this experiment, the cell was charged at 20 °C and discharged at a specific temperature. To describe capacity retention at various temperatures, we used the term "relative capacity", which was defined as the ratio of the capacity at a specific temperature to that obtained at 20 °C. It is shown that when the temperature is higher than −10 °C, the cell can be cycled reasonably and the temperature has little impact on the capacity. However, when the temperature goes below −20 °C, the cycling performance of the cell is significantly reduced. This phenomenon is probably associated with a substantial drop in the diffusivity of Li$^+$ ions within graphite as the temperature goes lower than −20 °C [19].

Discharge curves of the MGE Li-ion cell at various currents are plotted in Fig. 10. In this evaluation, the same charge conditions were applied to all cycles. The cell was charged to 4.3 V at a constant current of 1.1 mA (0.5C) and then kept at 4.3 V until the current fell to 0.11 mA (C/20). We see that the cell delivered reasonable capacity only at discharge currents of lower than 2 mA (∼0.9C) in spite of the high conductivity and good adhesion of the MGE to the electrodes. The thickness of the MGE was determined to be 0.14 mm, which is about five times higher than that of the com-
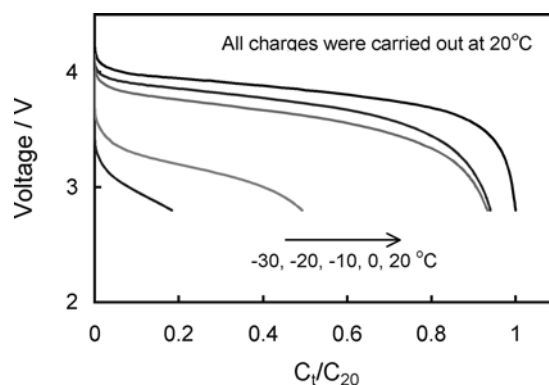

Fig. 8 Nyquist plots of the MCMB/MGE/LiMn$_2$O$_4$ cell for different storage times at 60 °C, which were recorded by keeping the cell at a constant 4.2 V for storage and applying a dc-bias of 4.2 V for measurement

Fig. 9 Discharge curves of the MCMB/MGE/LiMn$_2$O$_4$ cell at low temperatures, which were recorded at a discharge current of 0.62 mA (0.28C)
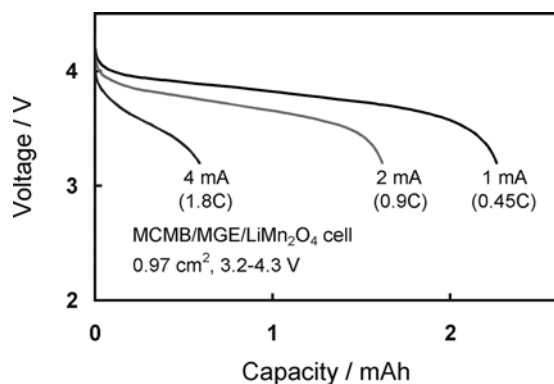
Fig. 10 Discharge curves of the MCMB/MGE/LiMn$_2$O$_4$ cell at various currents

mercial Celgard membrane. Based on this fact, we speculate that reducing the thickness of the microporous membrane and reducing the electrode loading of the active materials should be two effective approaches in improving the cycling performance of the MGE Li-ion batteries at high current rate and at low temperature. This speculation has been confirmed by a significant improvement in the cycling performance for the cells that used the same MGE technique but Saft's standard electrodes, which are known to have lower electrode loading [11].

Conclusions

Microporous gel electrolyte (MGE) has high ionic conductivity and good mechanical strength over a wide temperature range. In addition, the MGE is stable with respect to the low reductive potentials and to the high oxidative potentials, both of which are often reached during charging and storing of the Li-ion batteries. For battery application at elevated temperatures, MGE has significant advantages over the conventional gel polymer electrolyte. More importantly, the ease of MGE preparation provides a convenient approach for the fabrication of polymer Li-ion batteries.

References

1. Slane S, Salomon M (1995) J Power Sources 55:7
2. Appetecchi GB, Romagnoli P, Scrosati B (2001) Electrochem Commun 3:281
3. Prosini PP, Villano P, Carewska M (2002) Electrochim Acta 48:227
4. Denton I, Frank R (1999) US Patent 5,962,168
5. Kim DW, Oh B, Park JH, Sun YK (2000) Solid State Ionics 138:41
6. Du Pasquier A, Zheng T, Amatucci GG, Gozdz AS (2000) In: 198th Meeting of the Electrochemical Society, Phoenix, AZ, 22–27 October 2000, Abstract No 112
7. Christie AM, Christie L, Vincent CA (1998) J Power Sources 74:77
8. Abraham KM, Choe HS, Pasquariello DM (1998) Electrochim Acta 43:2399
9. Gozdz AS, Schmutz C, Tarascon JM, Warren P (1995) US Patent 5,418,091
10. Tarascon JM, Gozdz AS, Schmutz C, Shokoohi F, Warren PC (1996) Solid State Ionics 86–88:49
11. Zhang SS, Xu K, Foster DL, Ervin MH, Jow TR (2004) J Power Sources 125:114
12. Magistris A, Mustarelli P, Parazzoli F, Quartarone E, Piaggio P, Bottino A (2001) J Power Sources 97–98:657
13. Kim DW, Noh KA, Min HS, Kang DW, Sun KY (2002) Electrochem Solid St 5:A63
14. Stropnik C, Kaiser V (2002) Desalination 145:1
15. Jang DH, Shin YJ, Oh SM (1996) J Electrochem Soc 143:2204
16. Xia Y, Zhou Y, Yoshio M (1997) J Electrochem Soc 144:2593
17. Yamada A, Tanaka M (1995) Mater Res Bull 30:715
18. Thackeray MM, Yang SH, Kahaian AJ, Kepler DK, Skinner E, Vaughey JT, Hackney SA (1998) Electrochem Solid State Lett 1:7
19. Zhang SS, Xu K, Jow TR (2002) Electrochem Acta 48:241